Short-range Molecular Rearrangements in Ion Channels Detected by Tryptophan Quenching of Bimane Fluorescence

Leon D. Islas and William N. Zagotta

Department of Physiology and Biophysics, Howard Hughes Medical Institute, University of Washington, Seattle, WA 98195

Ion channels are allosteric membrane proteins that open and close an ion-permeable pore in response to various stimuli. This gating process provides the regulation that underlies electrical signaling events such as action potentials, postsynaptic potentials, and sensory receptor potentials. Recently, the molecular structures of a number of ion channels and channel domains have been solved by x-ray crystallography. These structures have highlighted a gap in our understanding of the relationship between a channel's function and its structure. Here we introduce a new technique to fill this gap by simultaneously measuring the channel function with the inside-out patch-clamp technique and the channel structure with fluorescence spectroscopy. The structure and dynamics of short-range interactions in the channel can be measured by the presence of quenching of a covalently attached bimane fluorophore by a nearby tryptophan residue in the channel. This approach was applied to study the gating rearrangements in the bovine rod cyclic nucleotide-gated ion channel CNGA1 where it was found that C481 moves towards A461 during the opening allosteric transition induced by cyclic nucleotide. The approach offers new hope for elucidating the gating rearrangements in channels of known structure.

INTRODUCTION

With the recent unveiling of many high-resolution x-ray crystallographic structures of ion channel proteins, we have entered a new era in ion channel research (Hille, 2001; Swartz, 2004). We are no longer asking simply what does the channel look like but instead are now asking how does the channel structure change or rearrange during gating. Gating is the process by which all ion channels control the opening and closing of their ion-permeable pore. In most cases it is thought to be an allosteric conformational change that is regulated by signals such as changes in transmembrane voltage, the binding of external or internal ligands, or membrane stretch (Sigworth, 1994; Li et al., 1997; Perozo and Rees, 2003). In each case, the regulator differentially affects the energy of the closed and open conformations and produces changes in the channel open probability. These changes in open probability are of fundamental importance to the physiological function of ion channels, but their detailed molecular mechanisms remain unknown.

Unfortunately, structural determination of the same channel protein in different conformational states has proven difficult. As a result, a number of methods have been developed to infer conformational changes from more indirect measurements such as gating effects of channel mutations, state-dependent changes in cysteine accessibility or disulfide bond formation, changes in cysteine-linked biotin accessibility, and state dependence of channel modulators and blockers

(Holmgren et al., 1997; Liu et al., 1997; Johnson and Zagotta, 2001; Laine et al., 2003; Phillips et al., 2005; Ruta et al., 2005). Recently, site-specific fluorescence labeling of channels has been used to follow the conformational changes associated with gating in voltage-dependent channels (Mannuzzu et al., 1996; Cha and Bezanilla, 1997; Cha et al., 1999; Zheng and Zagotta, 2000; Posson et al., 2005). The fluorescence of a fluorophore can report changes in local environment, accessibility to soluble quenchers, or proximity to nearby fluorophores by fluorescence resonance energy transfer (FRET) (Selvin, 1995). This method can be combined with whole-cell (or whole-oocyte) recording or excised patch recording, allowing simultaneous monitoring of channel function and structure with a relatively noninvasive probe.

The existing fluorescence methods have a number of limitations that have reduced their usefulness: (a) the cause of fluorescence changes is often ambiguous, and its time course often complex, making the molecular interpretation of the results difficult; (b) the fluorophores are often large (e.g., GFP derivatives) or attached by long linkers, making the fluorophore a poor reporter of the movement of its attachment point; (c) the fluorescent labeling is not always completely specific to the channel or the cysteine in question; (d) distances reported by standard FRET are too large

---

Abbreviations used in this paper: CNBD, cyclic nucleotide-binding domain; CNG, cyclic nucleotide-gated; FRET, fluorescence resonance energy transfer; HCN, hyperpolarization-activated cyclic nucleotide-modulated; NEM, *N*-ethylmaleimide; PCF, patch-clamp fluorometry.

Correspondence to William N. Zagotta: zagotta@u.washington.edu

(30–70 Å), on the order of the diameter of the channel protein itself; and (e) the distance dependence of FRET is extremely steep (FRET efficiency depends on the sixth power of the distance), making it sensitive to movements only in a very narrow range of distances, around R_o. This steep distance dependence, combined with orientation dependence and inaccuracies in measuring the FRET efficiency, makes distance measurements with FRET unreliable. The availability of high resolution structural information has created the need for a fluorescence approach that utilizes smaller, more specific, probes that monitor much shorter distances, on the order of the interaction distances observed in the molecular structures.

The need for a new approach is perhaps nowhere better illustrated than in cyclic nucleotide-gated (CNG) channels. CNG channels have been well characterized both functionally and structurally (Kaupp and Seifert, 2002; Craven and Zagotta, 2005). They are nonselective cation channels that are opened by the direct binding of cyclic nucleotides to an intracellular domain and have important roles in signal transduction, both in photoreceptors and olfactory neurons. Recently, a high resolution x-ray structure has been solved for the intracellular carboxy-terminal region of a related channel, the hyperpolarization-activated cyclic nucleotide-modulated (HCN) channel (Zagotta et al., 2003). This structure is in all likelihood very similar to the corresponding region in CNG channels. The availability of this structure has raised a number of important questions. (a) Does the structure of the isolated HCN fragment reflect a conformation of the intact HCN and CNG channels? (b) If so, which conformation does it represent: closed channel? Open channel? Gating intermediate? (c) And how does this structure rearrange during gating? These questions can be addressed by directly measuring the structure and dynamics of short-range molecular interactions predicted by the structure. Here we report a new method for simultaneously measuring short-range interactions with fluorescence spectroscopy and channel function with patch-clamp recording, and show an example of its use in CNG channels.

MATERIALS AND METHODS

Bimane-C3-maleimide and mono bromo bimane were purchased from Molecular Probes and dissolved at 100 mM in DMSO. This stock was aliquoted in small volumes and maintained frozen at −20°C. An aliquot was thawed just before each experiment and generally used for no more than two freeze–thaw cycles. All other reagents were obtained from Sigma-Aldrich.

Channel Mutagenesis
The CNGA1 channel with all seven endogenous cysteines removed (cysteineless) was used as a template for mutagenesis (Matulef et al., 1999). C481, I600C, and all tryptophan mutations were constructed by PCR mutagenesis as previously described (Gordon and Zagotta, 1995). All constructs were in the pGEMHE oocyte expression vector, and mRNA was prepared using the mMessage mAchine kit (Ambion). *Xenopus* oocytes were prepared and injected with RNA as previously described (Gordon and Zagotta, 1995).

Electrical Recording and Solutions
Current recording was performed in inside-out patches (Hamill et al., 1981) formed at the tip of 300–500 KΩ glass pipettes using an Axopatch 200B amplifier (Axon Instruments). Macroscopic currents were filtered at 2.5 KHz, sampled at 5 KHz, and digitized by an ITC-18 interface (Instrutech Co.). Data were acquired and analyzed with Pulse (HEKA Elektronik) and Igor (Wave Metrics). Patches were perfused with cyclic nucleotide-containing solutions using a rapid solution changer (BioLogic) in the presence of constant bath perfusion. The pipette and bath solutions contained 130 mM NaCl, 3 mM HEPES, 0.2 mM EDTA, pH 7.2 with NMG. Sodium salts of cyclic nucleotide were dissolved in this solution, compensating to maintain a 130 mM final sodium concentration. Immediately before the experiment, bimane maleimide was diluted to the desired concentration (indicated in figure legends) in this solution, with or without 2 mM cGMP.

Optical Recording Setup
Optical recordings in cell-free patches (patch-clamp fluorometry [PCF]) were performed on a Nikon Eclipse TE2000-E microscope equipped with a 60× 1.4 na Plan Apo oil immersion objective (Nikon). Laser illumination was achieved using a Coherent Radius solid-state laser (403 nm, 30 mW), coupled via an optical fiber to the total internal reflection (TIR) module from Nikon. The laser input power at the back aperture of the objective was 2.1 mW. In some experiments, this was attenuated to 0.26 mW using a neutral density filter to reduce photobleaching. No excitation filter was used. Light was collected by the objective, passed through a dichroic mirror centered at 405 nm and a long pass filter centered at 415 nm (Chroma Technology), and then was reflected on to the grating of a spectrograph (Acton MicroSpec 2150i) that was coupled to one of the side ports of the microscope. Light was detected by a Cascade 512B intensified CCD camera with a chip size of 512 × 512 pixels (Roper Scientific).

Spectroscopic measurements were done by placing the slit of the spectrograph over the image of the patch at the tip of the pipette and reflecting the image onto the grating (300/500 blazing). This produces a "spectral image" at the camera in which the x axis is a wavelength dimension and the y axis is a spatial dimension. The spectral region resolved by this grating and camera combination is 153 nm. Images were acquired for 300 ms to 1 s and the pixels were binned up to 5 × 5. The resolution is dependent on the level of binning of images and its value is 0.303 nm/pixel without binning.

Calibration of the spectrograph was achieved by generating a spectrum from a multi-line Ar-ion laser (SpectraPhysics) and mapping the peak wavelengths (456, 488, and 514 nm) to pixel number.

For imaging, the grating was moved to its zeroth-order position and the slit removed. Image acquisition and analysis, and microscope and instrument control were performed with MetaMorph (Universal Imaging Co.).

Data Analysis
Normalized dose responses of currents as a function cGMP concentration were fitted with the Hill equation:

$$\frac{I}{I_{max}} = \frac{1}{1 + \left[\frac{K_d}{[\text{cGMP}]}\right]^n}, \tag{1}$$
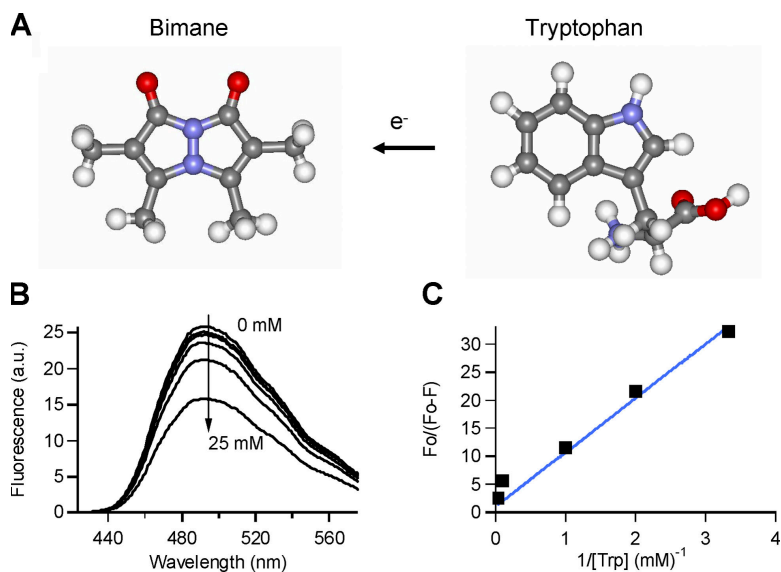
Figure 1. Mechanism of bimane fluorescence quenching by tryptophan. (A) Schematic of the electron transfer from tryptophan to bimane upon bimane excitation. The arrow represents donation of an electron from tryptophan to excited bimane. (B) Emission spectra of a 100 μM solution of bimane in increasing concentrations of tryptophan, indicated by the arrow. The reduction of the peak intensity is caused by tryptophan quenching. (C) Stern-Volmer analysis of the data in B. The straight line is a fit to the data with Eq. 3; the quenching constant $K = 0.083$ mM^{-1}.

where I is the cGMP-elicited current, I_{max} is the maximal current, K_d is the concentration of cGMP for which $I/I_{max} = 0.5$, and n is the Hill coefficient. Results from multiple experiments are expressed as the mean ± SEM. The time course of modification in the open state was fit with the following equation:

$$\frac{I_{cAMP}}{I_{cGMP}} = R_{max}(1 - e^{-kt})^m,$$ (2)

where I_{cAMP} and I_{cGMP} are the current in saturating cAMP and GMP, respectively. R_{max} is the steady-state fractional activation by cAMP, k is the modification rate, and m is an exponent that accounts for the sigmoidal time course.

Images and line scans from spectra were acquired in MetaMorph and transferred to Igor (Wave Metrics) for further analysis. Currents were analyzed in PulseFit (HEKA) and also transferred to Igor. Spectra were background corrected by subtracting a line scan of the nonfluorescent region immediately above the pipette. All the vertical pixels corresponding to the length of the patch were averaged to form a spectrum.

Quenching of bimane fluorescence (F) by tryptophan in solution was quantified from spectra by plotting the average fluorescence in a 7-nm window centered at 488 nm as a modified Stern-Volmer plot. Quenching of bimane in solution and in patches containing cysteineless CNGA1 channels were fit by a Stern-Volmer equation:

$$\frac{F_o}{F_o - F} = 1 + \frac{1}{[q]K},$$ (3)

where F_o is the fluorescence in the absence of quencher, F is the fluorescence at each concentration of quencher, K is the quenching constant, and $[q]$ is the concentration of tryptophan. Data for quenching of bimane in patches containing C481 or I600C channels were fit by a two component Stern-Volmer equation:

$$\frac{F_o}{F_o - F} = \frac{1}{1 - \left(\frac{f}{1+[q]K_1} - \frac{1-f}{1+[q]K_2}\right)},$$ (4)

where f is a number between 0 and 1 representing the relative contribution of each component, and K_i is the quenching constant for each component.

RESULTS

Tryptophan Quenches the Fluorescence of Bimane

Bimane is a small, environmentally sensitive fluorophore whose fluorescence has been used as a sensor of the local environment of residues in proteins (Kosower et al., 1979; Kosower et al., 1980; Kachel et al., 1998; Mansoor et al., 1999; Silvius, 1999). More recently it was discovered that bimane fluorescence is quenched by nearby tryptophan residues (Fig. 1 A) (Mansoor et al., 2002). Tryptophan quenching of bimane fluorescence is thought to be due to photo-induced electron transfer from tryptophan to excited bimane, and can be easily observed in a fluorometer with increasing concentrations of tryptophan added to the solution (Fig. 1 B). The decrease in fluorescence emission with increasing tryptophan concentration followed a simple linear Stern-Volmer relation, a plot of the inverse of the fractional fluorescence change as a function of the inverse of the quencher concentration (Fig. 1 C, see Materials and methods). This indicates that the quenching can be described by a single quenching constant K.

Mansoor et al. (2002) have shown that intramolecular quenching between bimane and tryptophan can be observed in T4 lysozyme, and the quenching occurs when the tryptophan to bimane distance is <15 Å. Thus, tryptophan quenching of bimane can be used as a proximity detector for distance changes associated with conformational changes in proteins (Mansoor et al., 2002; Janz and Farrens, 2004). Since the distances are much shorter than standard FRET, this approach, in theory, could allow one to compile a series of contact points between different regions of the protein and measure the dynamics of these contacts, akin to spin–spin coupling in EPR or NOE's in NMR. Unlike these other techniques, though, tryptophan quenching of bimane can be measured for
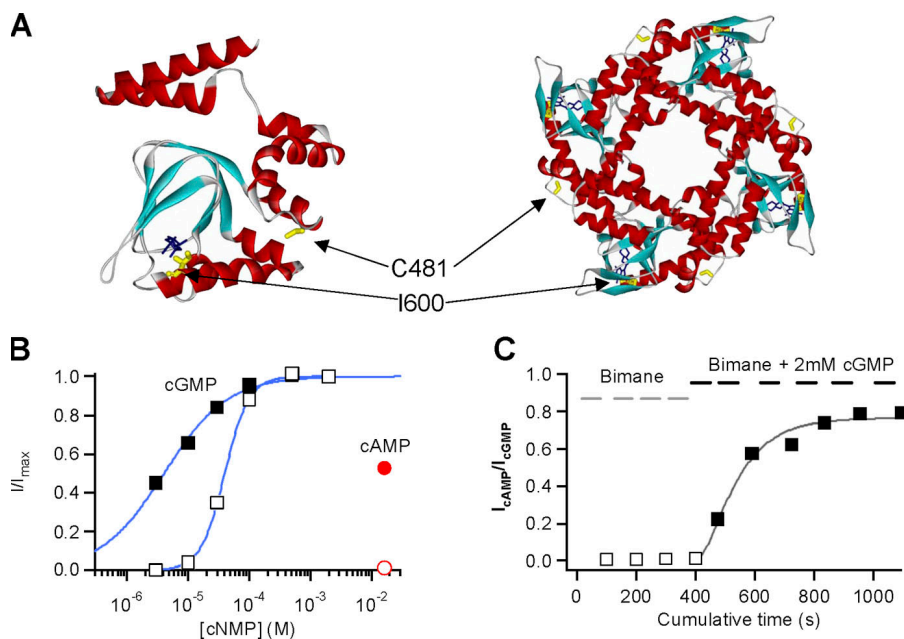
Figure 2. Characteristics of the C481 mutation. (A) Location of residues C481 and I600 in a homology model of the CNGA1 carboxy-terminal region based on the x-ray crystal structure of HCN2. (B) Cyclic nucleotide dose–response relations of unmodified and modified channels. Open squares are the cGMP dose–response data before modification. The smooth curve is a fit of Eq. 1 with $K_d = 40$ μM and $n = 2.2$. The open circle is the response to 16 mM cAMP, before modification. Closed squares are the cGMP dose–response data of the same patch after complete modification with 250 μM bimane maleimide in the presence of 2 mM cGMP. The data were fit with Eq. 1, with $K_d = 4.0$ μM and $n = 0.84$. The closed circle is the response to 16 mM cAMP after modification. (C) Time course of C481 modification by 400 μM bimane maleimide. Application of bimane maleimide in the absence or in the presence of 2 mM cGMP is indicated by the gray and black bars, respectively. Modification, as measured by the potentiation of the current in 16 mM cAMP relative to the current in 2 mM cGMP, occurs exceedingly slowly in closed channels (open squares), but proceeds with a rate constant of 29 ± 3.9 $M^{-1}s^{-1}$ ($n = 3$) in open channels (solid squares). The smooth line is a fit of Eq. 2 with a rate $k = 0.0098$ s^{-1} and $m = 2$.

very small amounts of channel protein in membrane patches simultaneous with electrical recording.

To explore the use of this approach to measure the conformational dynamics of an ion channel, we chose to study the gating rearrangements of the carboxy-terminal region of CNGA1 channels. This region exhibits 47% sequence similarity to the corresponding region of HCN2 channels whose structure was recently solved by x-ray crystallography (Zagotta et al., 2003). The structure consists of a fourfold symmetric tetramer on the intracellular end of the channel pore (Fig. 2 A). Each subunit contains a cyclic nucleotide-binding domain (CNBD), with bound cAMP (or cGMP), attached to the inner helices of the pore by an α-helical C-linker domain.

To get at the molecular dynamics of the channel, we have used patch-clamp fluorometry (PCF) to simultaneously measure the channel structure with fluorescence and the channel function with patch-clamp recording (Zheng and Zagotta, 2000, 2003). In our present PCF experiments, cysteines and tryptophans were introduced into the channel sequence and the mutant channels expressed in *Xenopus* oocytes. Then, inside-out patch-clamp recordings were made and the cysteine was modified with a cysteine-reactive bimane. This configuration allowed the time course of modification to be followed and the unincorporated fluorophore to be washed away. The fluorescence from the patch during various experimental manipulations could then be collected by a high numerical aperture objective and either imaged on a CCD camera or analyzed on a spectrograph to measure the emission spectrum.

Modification of C481 Channels with Bimane Maleimide

In CNGA1, an endogenous cysteine, C481, resides on the periphery of the carboxy-terminal region at the junction between the C-linker and CNBD domains (Fig. 2 A). We chose this cysteine residue as a site to introduce cysteine-reactive bimane into otherwise cysteine-less CNGA1 channels. Based on the effects and state dependence of cysteine-modifying reagents, this cysteine has previously been proposed to undergo a rearrangement during gating (Gordon et al., 1997; Brown et al., 1998). Fig. 2 B shows the gating effect of modifying C481 with bimane maleimide. Modification caused an increase in the apparent affinity for cGMP (K_d decreased from 34.0 ± 5.2 μM to 7.05 ± 6.11 μM, $n = 4$) (Fig. 2 B) and an increase in the fractional activation of the partial agonist cAMP (I_{cAMP}/I_{cGMP} increased from 0.0087 ± 0.0047 to 0.526 ± 0.075, $n = 3$) (Fig. 2 B). These results can both be explained if modification causes a decrease in the free energy of channel opening, making cAMP a better agonist, and suggest that C481 or nearby regions undergo a rearrangement during gating. Consistent with this interpretation, the rate of modification of C481 was profoundly state dependent. Addition of bimane maleimide in the absence of cGMP (closed state) caused little or no modification of the channels, while addition in the presence of cGMP (open state) caused a large increase in the cAMP-activated current (Fig. 2 C). These results suggest that C481 is more accessible in the open state.

After modification of C481 with bimane maleimide, bright fluorescence could be observed confined to the
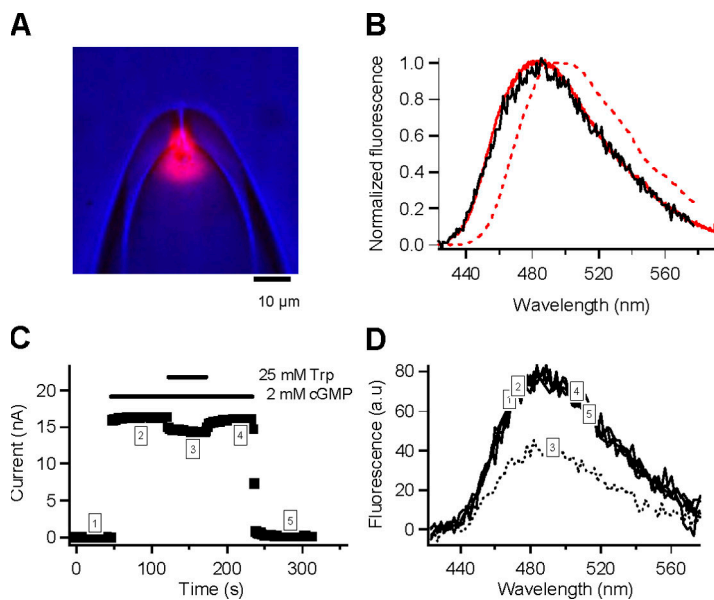
Figure 3. Spectroscopy of bimane-labeled C481 channels in patches. (A) Fluorescence image of an inside-out patch expressing C481 channels after modification with bimane maleimide. The fluorescence image is superimposed on a transmitted light image of the patch pipette. This patch contained 11 nA of cGMP-activated current, at 30 mV. (B) Emission spectrum of bimane in a patch similar to A (continuous black trace). The continuous red trace is the normalized emission spectrum of a solution of bimane maleimide–modified BSA. The dashed trace represents the emission spectrum of bimane maleimide in aqueous solution. (C) Time course of the amplitude of current elicited by 30-mV depolarizing pulses during application of 2 mM cGMP. Application of tryptophan produces a $12.7 \pm 0.2\%$ ($n = 3$) reversible blockade of current. (D) Emission spectra of the patch in C acquired at the times indicated by numbers. Tryptophan produces a 40% reduction in fluorescence that is completely reversible (trace 3, dotted line). There is no difference in the fluorescence of open channels (traces at times 2 and 4) and closed channels (traces at times 1 and 5).

area of the patch (Fig. 3 A). With excitation by a 403-nm laser, an omega-shaped patch was clearly visible inside the pipette. Unlike most fluorophores, bimane maleimide shows a marked increase in fluorescence quantum yield upon reaction with a cysteine (Kosower et al., 1980), suggesting that most of the observed fluorescence arose from cysteine-reacted bimane. Consistent with this idea, little or no fluorescence was observed in patches previously blocked by 10 min in 1 mM *N*-ethylmaleimide (NEM) in the presence of cGMP (unpublished data). Spectral analysis of the fluorescence revealed that the emission spectrum of bimane was slightly blue shifted ($\sim$10 nm; Fig. 3 B, black trace) relative to the spectrum of free bimane in solution (Fig. 3 B, dashed red trace) and similar to bimane reacted with BSA (Fig. 3 B; solid red trace). Bimane has been extensively used as an environmentally sensitive fluorophore, and the blue shift is as would be expected for bimane experiencing the less polar environment of a protein (Wang et al., 1997; Mansoor et al., 1999).

Since the fluorescently labeled channels are present in the controlled environment of an inside-out patch, we could directly measure the effects of exogenously applied cyclic nucleotide and tryptophan in solution on channel ionic current and fluorescence. 2 mM cGMP, a saturating concentration, produced a large increase in the current (Fig. 3 C, corresponding to the activation of $\sim$15,000 channels) but no detectable change in the fluorescence (Fig. 3 D, compare spectra 1 and 2). This result indicates that, at this concentration, cGMP has no direct effect on the fluorescence of bimane. The addition of 25 mM tryptophan produced only a small decrease in current (Fig. 3 C) but a large decrease in fluorescence (Fig. 3 D, compare spectra 2 and 3). The decrease in fluorescence was rapidly reversible

(Fig. 3 D, compare spectra 3 and 4) and reflects the quenching of immobilized bimane by tryptophan in solution.

The quenching efficiency of tryptophan in solution was state dependent. Fig. 4 A shows Stern-Volmer plots for the quenching of bimane in a C481-containing patch in the absence (filled squares) and presence (open squares) of cGMP. A decreased slope in these plots reflects a higher quenching efficiency (a higher quenching constant K). Therefore C481-bimane was more easily quenched by soluble tryptophan, and thus more accessible in the open state in the presence of cGMP ($K = 6.1 \pm 1.5$ mM^{-1}, $n = 3$) than in the closed state in the absence of cyclic nucleotide ($K = 2.8 \pm 1.1$ mM^{-1}, $n = 3$). The opposite state dependence occurs upon labeling a cysteine introduced at the 600 position (I600C). I600C is located in the C-helix of the CNBD of CNGA1 (Fig. 1 A) and has been shown previously to form a homotypic intersubunit disulfide bond in closed channels (Matulef and Zagotta, 2002). Unlike C481, I600C-bimane was more accessible to tryptophan in solution in the closed state ($K = 1.55 \pm 0.45$ mM^{-1}, $n = 2$) than in the open state ($K = 0.63 \pm 0.08$ mM^{-1}, $n = 2$) (Fig. 4 B), consistent with the proposed movement of the C-helix during CNG channel gating (Goulding et al., 1994; Varnum et al., 1995). In both cases, data could not be fit by a simple linear Stern-Volmer relation, but required two quenching components. The state-dependent component was only a fraction of the total patch fluorescence (15% for C481 and 20% for I600C in Fig. 4, A and B, respectively). This component clearly arises from channel-associated fluorophore, suggesting that under these labeling conditions, only a fraction of the bimane in the patch was directly associated with the channel. The state-independent component probably represents background fluorescence
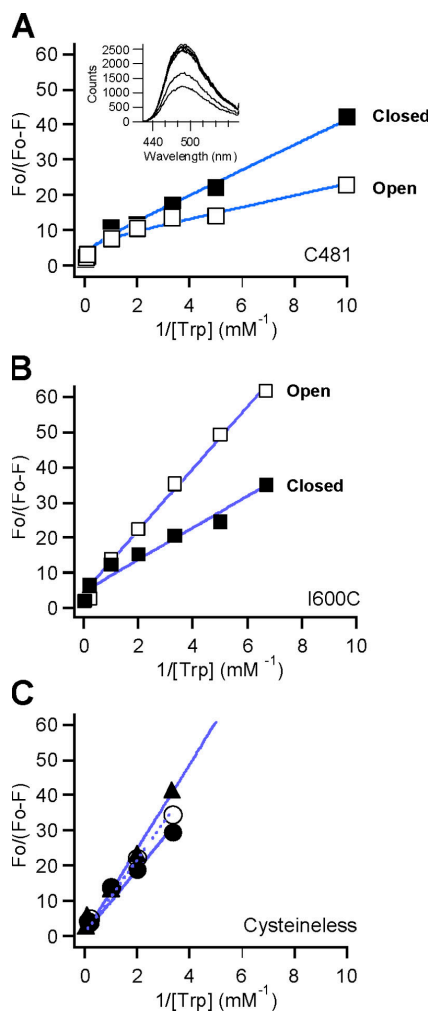
Figure 4. Quantification of bimane fluorescence quenching by applied tryptophan in solution. (A) Stern-Volmer plot analysis of a bimane maleimide–modified patch expressing C481 channels. Tryptophan quenching is more effective in the open state than in the closed state. The curves are fits of Eq. 4 with values: (closed) $f = 0.15$, $K_1 = 1.72$ mM^{-1}, and $K_2 = 0.026$ mM^{-1}; (open) $f = 0.15$, $K_1 = 3.73$ mM^{-1}, and $K_2 = 0.025$ mM^{-1}. The inset shows the patch emission spectra at different concentrations of tryptophan. (B) Quenching characteristics of I600C channels. Quenching is more effective in the closed state than in the open state. The curves are fits of Eq. 4 with values: (closed) $f = 0.20$, $K_1 = 1.092$ mM^{-1}, and $K_2 = 0.0052$ mM^{-1}; (open) $f = 0.20$, $K_1 = 0.55$ mM^{-1}, and $K_2 = 0.0061$ mM^{-1}. (C) Tryptophan quenching of a bimane-labeled inside-out patch containing cysteineless CNGA1 channels in the presence of 2 mM cGMP (open circles) and in the absence of nucleotides (closed circles). Smooth curves are fits of Eq. 3 with values: (closed) $K = 0.11$ mM^{-1}; (open) K $= 0.096$ mM^{-1}. Quenching of bimane maleimide in solution is represented by the triangles. The quenching constant K is 0.083 mM^{-1}.
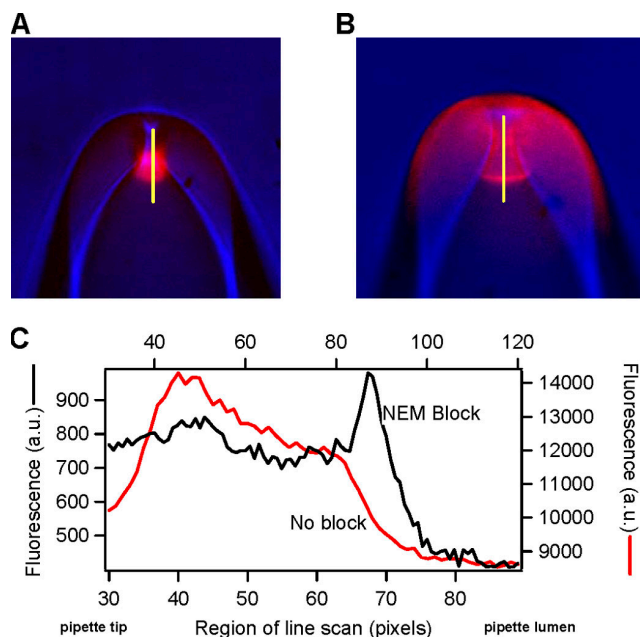
Figure 5. Components of patch fluorescence. (A) Fluorescence emission image of a patch expressing C481 channels modified with bimane maleimide without NEM block. The yellow line indicates the region used in the scan in C. The exposure to the 405-nm laser was 300 ms. (B) A patch expressing C481 channels modified after cysteine block with 1 mM NEM for 4 min in the closed state. The exposure was 1 s, with eight times the laser intensity used in A. (C) Line scans of the images in A and B.

thalium quenching of other fluorophores attached at C481 (Zheng and Zagotta, 2000, 2003). The reason for this increased quenching efficiency is unknown.

Although the state dependence of quenching provided a useful way to distinguish between background fluorescence and channel-associated fluorescence, we sought an additional approach to improve the specificity of bimane labeling. We capitalized on the state-dependent accessibility of C481 to eliminate much of the nonchannel-associated fluorescence. By applying a nonfluorescent cysteine-modifying reagent in the absence of cGMP, we first blocked reactive cysteines in the patch that were accessible when the channels were closed. We could then specifically label the channels with bimane maleimide in the presence of cGMP. The results of such an experiment are shown in Fig. 5. Labeling the patch without blocking produced a fairly uniform labeling throughout the area of the patch (Fig. 5 A, and red trace in Fig. 5 C). However blocking the background first for 7 min with 1 mM NEM in the absence of cyclic nucleotide produced more specific labeling of the plasma membrane as seen by the bright signal in the area of the membrane (Fig. 5 B) and by the now well-defined peak of fluorescence seen in the line scan (Fig. 5 C). Preblocking nonchannel-associated cysteines with NEM produced a specific reduction of fluorescence in the interior of the patch (note the different

and could be directly observed in patches containing cysteineless CNGA1 channels. Its quenching was similar to quenching of bimane free in solution (Fig. 4 C). Interestingly the quenching efficiency of the channel-associated component was higher than for free bimane. A similar observation has been made for iodide and
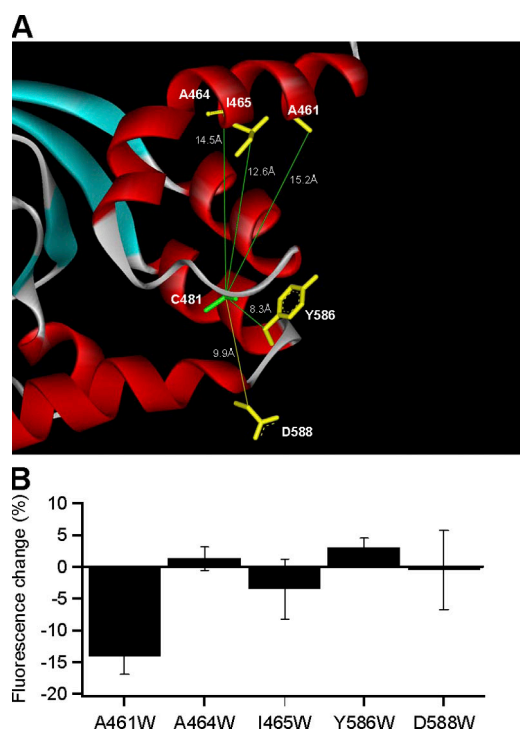
Figure 6. Location and quenching effects of tryptophan mutants. (A) Homology model of one subunit of the CNGA1 channel, showing the location of residues that were mutated to tryptophan. The numbering is that of the CNGA1 sequence. Distances to the α-carbon of C481 are indicated by green lines and are given in angstroms. (B) Quantification of the degree of state-dependent quenching of bimane in C481 produced by individual tryptophan residues. The bars represent the mean. The error bars are the SEM.

scales in Fig. 5 C), suggesting that most of the background fluorescence arose from cytosolic proteins that are associated with the patch. The rate of modification of the background sites is considerably faster than modification of C481 (Zheng and Zagotta, 2000, 2003), so the specificity of labeling can also be increased by blocking the background sites with short exposures to NEM, eliminating the need for state-dependent modification. However because fluorescence intensity changes of just a few percent could be easily observed, no background blocking was applied for the experiments to follow.

Intramolecular Quenching of Bimane by Introduced Tryptophan Residues

The real power of this new approach is not its ability to observe state-dependent changes in accessibility of residues to soluble quenchers, but in its ability to measure state-dependent changes in short-range interactions in the channel, using tryptophan as an intrinsic quencher in the channel. This is particularly valuable when a high-resolution structure is available that provides testable predictions and a framework within which to interpret the results. Such is the case for the CNG channel.

We used our homology model of the carboxy-terminal region of CNGA1 (Fig. 1 A) to identify residues within a sphere of 15 Å radius from C481. Five residues were chosen to be mutated to tryptophan in a C481 background and act as possible quenching partners for C481-bimane. Fig. 6 A shows the position of these five mutated residues, three in the D′ helix (A461W, A464W, and I465W) and two in the C helix (Y586W and D588W), and their corresponding β-carbon distances to C481. All of these channels with introduced tryptophan residues produced relatively large cGMP-activated currents in inside-out patches (>1000 pA at 30 mV) and could be modified by bimane maleimide at C481. However, most did not show state-dependent changes in bimane fluorescence that would reflect changes in intramolecular quenching by the introduced tryptophan (Fig. 6 B). One such mutant is D588W. After bimane modification of C481, D588W channels could be normally activated by cGMP (Fig. 7 A) and exhibited bimane fluorescence, but the fluorescence was not significantly different in the absence and presence of cGMP (Fig. 7 B, compare spectra 1 and 2).

In contrast, A461W channels showed a significant change in fluorescence upon application of cGMP (Fig. 7, C and D). 2 mM cGMP caused a 14.1 ± 2.9% ($n = 5$) decrease in fluorescence that was rapidly reversible and reproducible. The fluorescence quenching was only seen in the A461W mutant and was not observed in C481F-A461W channels. Furthermore, the quenching was not associated with a change in shape of the emission spectrum, but only a decrease in peak amplitude (Fig. 7 D) similar to quenching by soluble tryptophan. These results suggest that the quenching in A461W channels arose from intramolecular quenching of C481-bimane by A461W.

To confirm that the change in bimane quenching by A461W was due to the molecular rearrangement associated with CNG channel gating, we compared the cyclic nucleotide dependence of quenching to that of channel activation measured in the same patch. As shown in Fig. 8, the magnitude of the quenching exhibited the same dependence on cGMP (Fig. 8 B) as the activation of the modified A461W channel (Fig. 8 A). The dose dependence of quenching could be fit with the same apparent affinity (K_d) and Hill coefficient (n) as for activation of modified channels. Furthermore, 16 mM cAMP was similarly effective at promoting channel opening and quenching of C481 by A461W. 16 mM cAMP is a saturating concentration that should bind completely but is less able to promote channel opening. These results indicate that the fluorescence quenching of C481-bimane is reporting a molecular rearrangement of the channel associated with the opening gating transition and not cyclic nucleotide binding. The decrease in fluorescence with cGMP suggests that C481 moves closer to A461 during the activating allosteric transition in the channel.
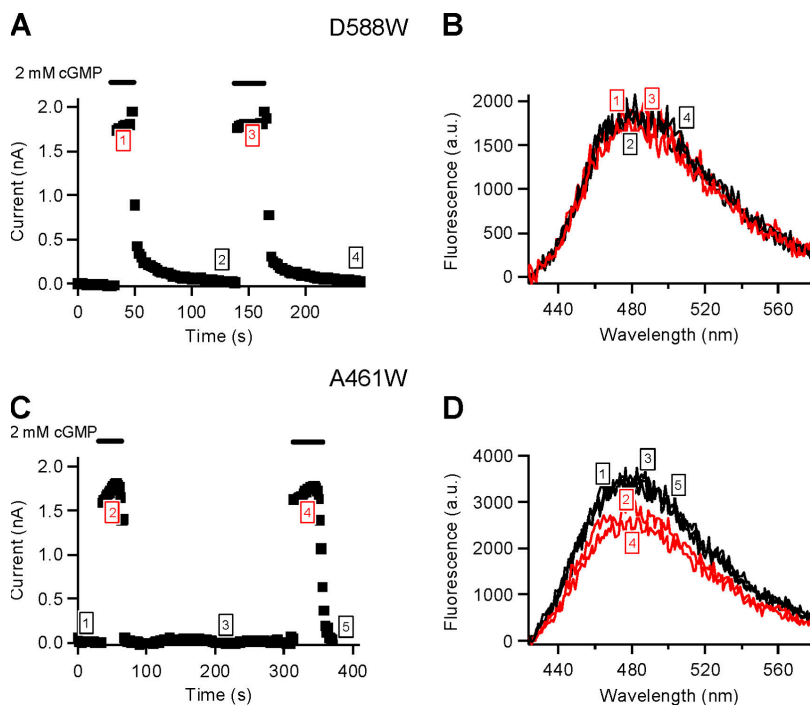
Figure 7. Fluorescence changes in tryptophan mutants. (A) Currents from D588W channels after bimane modification upon application of 2 mM cGMP elicited by pulses to 30 mV. (B) Spectra taken at the times indicated by the numbers in A. (C) Currents from A461W channels after bimane modification upon application of 2 mM cGMP elicited by pulses to 30 mV. (D) Spectra taken at the times indicated by the numbers in C. Red traces are the open channel emission spectra, and black traces are the closed channel emission spectra. Quenching of peak fluorescence in A461W channels upon opening is ~18%.

The bimane C_3-maleimide used in these experiments contains a relatively long linker between the bimane and maleimide moieties, leaving open the possibility that the quenching is not faithfully reporting the movement of C481 relative to A461W. To address this concern, we reacted C481, A461W channels with mono-bromobimane, which contains virtually no linker. As shown in Fig. 9, the open state-dependent quenching with monobromobimane modification was quantitatively very similar to that with bimane C_3-maleimide. These results confirm that the fluorescence quenching is reporting a movement of C481 relative to A461W during channel opening and does not require the long linker of bimane maleimide.

DISCUSSION

In this paper we have demonstrated a new approach to study conformational changes in channels using quenching of bimane fluorescence by nearby tryptophan residues. Fluorescence from bimane-modified channels is readily observable in inside-out patches and spectroscopic measurements are easily obtained. We observed that the fluorescence of bimane-modified channels can be quenched by both tryptophan in solution and tryptophan in the channel. The state-dependent fluorescence changes in the C481-bimane A461W channels are well correlated with the cyclic nucleotide–induced opening conformational change, indicating that the fluorescence is reporting a conformational change that is tightly coupled to channel opening. Our results explicitly rule out the possibility that the fluorescence is simply reporting cyclic nucleotide binding. (a) cAMP is a partial agonist and only partially quenches bimane fluorescence relative to cGMP. If it was the binding of the negatively charged ligand that caused quenching, then saturating concentrations of cAMP would produce the same degree of quenching as cGMP. (b) In our experiments with C481 channels with no additional tryptophan, we observe no fluorescence quenching effects, arguing that the ligand alone is not responsible for quenching.

The absence of a cyclic nucleotide–dependent change in bimane fluorescence in the other tryptophan mutants is difficult to interpret. These negative results could arise in at least three ways: (1) these tryptophans and bimane may not be close enough or properly oriented to produce quenching; (2) the distance between these tryptophans and C481 might not change enough during channel gating to change the quenching; and (3) the change in quenching might be too small to detect above the background bimane fluorescence. Given these uncertainties, it seems most prudent in this approach to interpret only the results from bimane–tryptophan pairs that produce a gating-dependent increase or decrease in bimane fluorescence, as seen in C481-bimane A461W. In the future, an instrument capable of measuring fluorescence lifetimes could be used to determine the absolute degree of quenching in each state of the channel, allowing a more thorough comparison to the x-ray structure.

It is interesting to note that of all of the residues we tested, A461W is the furthest from C481 (15 Å) in the homology model of the carboxy-terminal region.
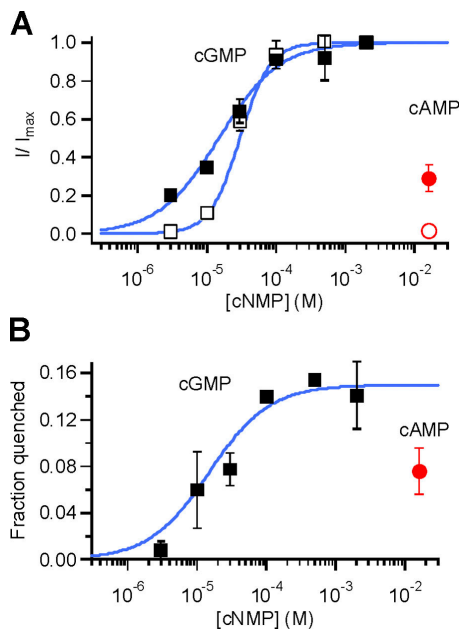
Figure 8. The cyclic nucleotide dependence of bimane quenching suggests that fluorescence reports a conformational change associated with channel opening. (A) Average cyclic nucleotide dose–response relations of unmodified and modified channels. Open squares are the cGMP dose–response data before modification. The smooth curve is a fit of Eq. 1 with $K_d = 30$ μM and $n = 2.0$. The open circle is the response to 16 mM cAMP, before modification. Closed squares are the cGMP dose–response data after modification. The data were fit with Eq. 1, with $K_d = 15$ μM and $n = 1.0$. The closed circle is the response to 16 mM cAMP after modification. (B) cGMP dose–response relation of bimane quenching in modified A461W channels. The data were fit with Eq. 1 with a maximum value of 0.15, and the same parameters used for the cGMP dose–response relation of modified channels in A. The red symbol is the quenching observed when the channels are opened by 16 mM cAMP and was corrected for the $3.1 \pm 0.6\%$ ($n = 3$) quenching of bimane produced by 16 mM cAMP alone.

This distance is on the outer limits of the distances reported for tryptophan to quench bimane (Mansoor et al., 2002). One possible explanation for this observation is that the crystallized structure of the carboxy-terminal region is in the resting conformation, at least with regard to the relative position of A461 and C481, and that the two residues are closer in the open channel. A similar proposal was recently made based on the effects of mutating salt bridges observed in the structure of the C-linker region (Craven and Zagotta, 2004). In both CNGA1 and HCN2 channels, mutating these salt bridges caused a potentiation of channel activation, suggesting that the salt bridges helped stabilize the closed conformation. Therefore the crystal structure of the C-linker region may reside in a resting configuration, and activation of the channel may move A461 and C481 in closer proximity. Alternatively, A461W and C481-bimane may be in close enough proximity in the structure to achieve quenching, and closure of the channel may move them even further apart. Data from more
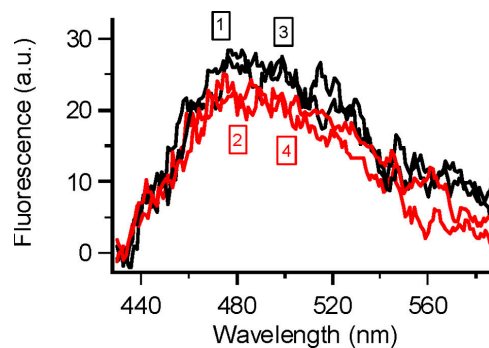

Figure 9. Fluorescence changes in A461W-C481 channels modified with 250 μM monobromobimane. After modification, spectra were acquired in the absence of cyclic nucleotide (closed state, black traces) or in the presence of 2 mM cGMP (open state, red traces) in the order indicated by the numbers in boxes. The amount of quenching in this experiment was 14.8%.

bimane–tryptophan pairs are needed to distinguish between these alternatives.

With multiple quenching pairs, tryptophan quenching of bimane fluorescence offers great hope for elucidating the rearrangements and dynamics of gating conformational changes in ion channels. This approach should prove generally useful for probing short-range interactions in proteins, especially when a structural framework exists for interpreting state-dependent changes in quenching as structural rearrangements. By focusing on short-range interactions, it overcomes many of the problems associated with intramolecular FRET experiments. In addition, only one fluorophore needs to be introduced into the channel by modification, significantly reducing the problems with specificity of introducing two separate fluorophores into the same protein. Finally, combined with the use of PCF, this approach allows for the study of intracellular sites, where many of the rearrangements in ion channels take place.

REFERENCES

Brown, R.L., S.D. Snow, and T.L. Haley. 1998. Movement of gating machinery during the activation of rod cyclic nucleotide-gated channels. *Biophys. J.* 75:825–833.

Cha, A., and F. Bezanilla. 1997. Characterizing voltage-dependent conformational changes in the Shaker K+ channel with fluorescence. *Neuron.* 19:1127–1140.

Cha, A., G.E. Snyder, P.R. Selvin, and F. Bezanilla. 1999. Atomic scale movement of the voltage-sensing region in a potassium channel measured via spectroscopy. *Nature.* 402:809–813.

Craven, K.B., and W.N. Zagotta. 2004. Salt bridges and gating in the COOH-terminal region of HCN2 and CNGA1 channels. *J. Gen. Physiol.* 124:663–677.

Craven, K.B., and W.N. Zagotta. 2006. CNG and HCN channels: two peas, one pod. *Annu. Rev. Physiol.* 68:375–401.

Gordon, S.E., and W.N. Zagotta. 1995. Localization of regions affecting an allosteric transition in cyclic nucleotide-activated channels. *Neuron.* 14:857–864.

Gordon, S.E., M.D. Varnum, and W.N. Zagotta. 1997. Direct interaction between amino- and carboxyl-terminal domains of cyclic nucleotide-gated channels. *Neuron.* 19:431–441.

Goulding, E.H., G.R. Tibbs, and S.A. Siegelbaum. 1994. Molecular mechanism of cyclic-nucleotide-gated channel activation. *Nature.* 372:369–374.

Hamill, O.P., A. Marty, E. Neher, B. Sakmann, and F.J. Sigworth. 1981. Improved patch-clamp techniques for high-resolution current recording from cells and cell-free membrane patches. *Pflugers Arch.* 391:85–100.

Hille, B. 2001. Ion Channels of Excitable Membranes. Third edition. Sinauer, Sunderland, MA. 814 pp.

Holmgren, M., P.L. Smith, and G. Yellen. 1997. Trapping of organic blockers by closing of voltage-dependent K$^+$ channels: evidence for a trap door mechanism of activation gating. *J. Gen. Physiol.* 109:527–535.

Janz, J.M., and D.L. Farrens. 2004. Rhodopsin activation exposes a key hydrophobic binding site for the transducin α-subunit C terminus. *J. Biol. Chem.* 279:29767–29773.

Johnson, J.P., Jr., and W.N. Zagotta. 2001. Rotational movement during cyclic nucleotide-gated channel opening. *Nature.* 412:917–921.

Kachel, K., J. Ren, R.J. Collier, and E. London. 1998. Identifying transmembrane states and defining the membrane insertion boundaries of hydrophobic helices in membrane-inserted diphtheria toxin T domain. *J. Biol. Chem.* 273:22950–22956.

Kaupp, U.B., and R. Seifert. 2002. Cyclic nucleotide-gated ion channels. *Physiol. Rev.* 82:769–824.

Kosower, N.S., E.M. Kosower, G.L. Newton, and H.M. Ranney. 1979. Bimane fluorescent labels: labeling of normal human red cells under physiological conditions. *Proc. Natl. Acad. Sci. USA.* 76:3382–3386.

Kosower, N.S., G.L. Newton, E.M. Kosower, and H.M. Ranney. 1980. Bimane fluorescent labels. Characterization of the bimane labeling of human hemoglobin. *Biochim. Biophys. Acta.* 622:201–209.

Laine, M., M.C. Lin, J.P. Bannister, W.R. Silverman, A.F. Mock, B. Roux, and D.M. Papazian. 2003. Atomic proximity between S4 segment and pore domain in Shaker potassium channels. *Neuron.* 39:467–481.

Li, J., W.N. Zagotta, and H.A. Lester. 1997. Cyclic nucleotide-gated channels: structural basis of ligand efficacy and allosteric modulation. *Q. Rev. Biophys.* 30:177–193.

Liu, Y., M. Holmgren, M.E. Jurman, and G. Yellen. 1997. Gated access to the pore of a voltage-dependent K+ channel. *Neuron.* 19:175–184.

Mannuzzu, L.M., M.M. Moronne, and E.Y. Isacoff. 1996. Direct physical measure of conformational rearrangement underlying potassium channel gating. *Science.* 271:213–216.

Mansoor, S.E., H.S. McHaourab, and D.L. Farrens. 1999. Determination of protein secondary structure and solvent accessibility using site-directed fluorescence labeling. Studies of T4 lysozyme using the fluorescent probe monobromobimane. *Biochemistry.* 38:16383–16393.

Mansoor, S.E., H.S. McHaourab, and D.L. Farrens. 2002. Mapping proximity within proteins using fluorescence spectroscopy. A study of T4 lysozyme showing that tryptophan residues quench bimane fluorescence. *Biochemistry.* 41:2475–2484.

Matulef, K., and W. Zagotta. 2002. Multimerization of the ligand binding domains of cyclic nucleotide-gated channels. *Neuron.* 36:93–103.

Matulef, K., G.E. Flynn, and W.N. Zagotta. 1999. Molecular rearrangements in the ligand-binding domain of cyclic nucleotide-gated channels. *Neuron.* 24:443–452.

Perozo, E., and D.C. Rees. 2003. Structure and mechanism in prokaryotic mechanosensitive channels. *Curr. Opin. Struct. Biol.* 13:432–442.

Phillips, L.R., M. Milescu, Y. Li-Smerin, J.A. Mindell, J.I. Kim, and K.J. Swartz. 2005. Voltage-sensor activation with a tarantula toxin as cargo. *Nature.* 436:857–860.

Posson, D.J., P. Ge, C. Miller, F. Bezanilla, and P.R. Selvin. 2005. Small vertical movement of a K+ channel voltage sensor measured with luminescence energy transfer. *Nature.* 436:848–851.

Ruta, V., J. Chen, and R. MacKinnon. 2005. Calibrated measurement of gating-charge arginine displacement in the KvAP voltage-dependent K+ channel. *Cell.* 123:463–475.

Selvin, P.R. 1995. Fluorescence resonance energy transfer. *Methods Enzymol.* 246:300–334.

Sigworth, F.J. 1994. Voltage gating of ion channels. *Q. Rev. Biophys.* 27:1–40.

Silvius, J.R. 1999. Fluorescence measurement of lipid-binding affinity and interbilayer transfer of bimane-labeled lipidated peptides. *Methods Mol. Biol.* 116:177–186.

Swartz, K.J. 2004. Towards a structural view of gating in potassium channels. *Nat. Rev. Neurosci.* 5:905–916.

Varnum, M.D., K.D. Black, and W.N. Zagotta. 1995. Molecular mechanism for ligand discrimination of cyclic nucleotide-gated channels. *Neuron.* 15:619–625.

Wang, Y., S.E. Malenbaum, K. Kachel, H. Zhan, R.J. Collier, and E. London. 1997. Identification of shallow and deep membrane-penetrating forms of diphtheria toxin T domain that are regulated by protein concentration and bilayer width. *J. Biol. Chem.* 272:25091–25098.

Zagotta, W.N., N.B. Olivier, K.D. Black, E.C. Young, R. Olson, and E. Gouaux. 2003. Structural basis for modulation and agonist specificity of HCN pacemaker channels. *Nature.* 425:200–205.

Zheng, J., and W.N. Zagotta. 2000. Gating rearrangements in cyclic nucleotide-gated channels revealed by patch-clamp fluorometry. *Neuron.* 28:369–374.

Zheng, J., and W.N. Zagotta. 2003. Patch-clamp fluorometry recording of conformational rearrangements of ion channels. *Sci. STKE.* 176:PL7.